Importance of C-2 Symmetry for the Device Performance of a Newly Synthesized Family of Fused-Ring Thiophenes

9 AUTHORS, INCLUDING:

Adama Tandia
Corning Incorporated
13 PUBLICATIONS **150** CITATIONS

SEE PROFILE

Hon Hang Fong
Shanghai Jiao Tong University
62 PUBLICATIONS **1,029** CITATIONS

SEE PROFILE

Vladimir A. Pozdin
University of Texas at Dallas
16 PUBLICATIONS **316** CITATIONS

SEE PROFILE

D.-M. Smilgies
Cornell University
261 PUBLICATIONS **5,520** CITATIONS

SEE PROFILE

Importance of C_2 Symmetry for the Device Performance of a Newly Synthesized Family of Fused-Ring Thiophenes

Mingqian He,*[†] Jianfeng Li,[†] Adama Tandia,[†] Michael Sorensen,[†] Feixia Zhang,[†] Hon Hang Fong,[‡] Vladimir A. Pozdin,[‡] Detlef-M. Smilgies,[§] and George G. Malliaras[‡]

[†]*Corning, Incorporated, SP-FR-6, Corning, New York 14830,* [‡]*Materials Science and Engineering, Cornell University, Ithaca, New York 14853, and* [§]*Cornell High Energy Synchrotron Source, Cornell University, Ithaca, New York 14853*

We investigated the relationship between molecular structure and field-effect hole mobility in a family of fused-ring polythiophene copolymers that we designed recently. The results suggest that a repeat unit that possesses a C_2-axis perpendicular to the conjugation plane is important to achieve a high mobility. Our finding is supported by a review of literature data. Many polymer semiconductors showing a hole or electron mobility of > 0.1 cm^2/(V s) feature a repeat unit with C_2 symmetry; however, exceptions have been found from some push−pull polymer structures.

Introduction

Polymer semiconductors are attracting a great deal of interest for applications in low-cost, large-area, and flexible active-matrix display backplanes, radio-frequency identification (RFID) tags, and chemical/biological sensors.[1−3] The development of regioregular poly(3-hexylthiophene) (P3HT)[4a−c] ushered in a new era in the design of soluble thiophene-based polymers with field-effect hole mobilities reaching the 0.1 cm^2/(V s) benchmark, making these materials competitive with amorphous silicon.[4d]

Since then, the performance of polymer semiconductors has experienced great improvement,[5] as various aspects of the repeat unit architecture are being intensively explored. For example, the reduction of the number of alkyl substituents on the thiophene backbone in poly(3,3″-diakyl-quarterthiophene)s (PQTs) was found to promote self-assembly and crystallization, resulting in a field-effect hole mobility up to 0.2 cm^2/(V s) after post-deposition annealing.[6] Another particularly noteworthy example are poly(2,5-bis(alkyl-thiophen-2-yl)thieno[3,2-b]thiophenes) (pBTTT), which feature an unsubstituted unit that consists of two fused thiophene rings.[7] The highly symmetric structure of the fused unit promotes the formation of crystalline regimes, so that the polymer main chains can assemble into large domains on crystallization from a liquid crystal phase. Field-effect hole mobilities of 0.2−0.6 cm^2/(V s) have been observed.[7] A third example is poly(2,5-bis(thiophene-2-yl)-(3,7-ditridecanyltetrathienoacene) (P2TDC13FT4), with a field-effect hole mobility exceeding 0.3 cm^2/(V s), which was achieved by increasing the rigidity of the thiophene monomer via the use of an alkyl-substituted core that consists of four fused-thiophene rings.[8]

Our current understanding of conjugated polymer design calls for a rigid and planar backbone, which will show extended π-conjugation along the main chain and promote close packing, allowing efficient intermolecular charge transfer.[9] It also calls for alkyl side chains with appropriate length to ensure solubility, arranged at appropriate density to allow dense packing and, at appropriate positions, to yield a regioregular polymer and ensure minimal defects in conjugation.[10] Additional design rules address stability, for example, in terms of limiting the conjugation length to improve oxidative stability of *p*-type materials.[11]

We recently reported a family of fused thiophene−bithiophene co-polymers, as materials of interest for thin-film transistor applications.[12] In particular, a comparison of

---

*Author to whom correspondence should be addressed. E-mail: hem@corning.com.

(1) Sirringhaus, H.; Tessler, N.; Friend, R. H. *Science* **1998**, *280*, 1741.
(2) Sirringhaus, H.; Ando, M. *MRS Bull.* **2008**, *33*, 676.
(3) Bao, Z. *Adv. Mater.* **2000**, *12*, 227.
(4) (a) McCullough, R. D.; Lowe, R. D. *J. Chem. Soc., Chem. Commun.* **1992**, 70. (b) McCullough, R. D.; Lowe, R. D.; Jayaraman, M.; Anderson, D. L. *J. Org. Chem.* **1993**, *58*, 904. (c) McCullough, R. D. *Adv. Mater.* **1998**, *10*, 93–116. (d) Bao, Z.; Dobabalapur, A.; Lovinger, A. J. *Appl. Phys. Lett.* **1996**, *69*, 4108.
(5) DeLongchamp, D. M.; Kline, R. J.; Lin, E. K.; Fisher, D. A.; Richter, L. J.; Lucas, L. A.; Heeney, M.; McCulloch, I.; Northrup, J. E. *Adv. Mater.* **2007**, *19*, 833.
(6) Ong, B. S.; Wu, Y.; Liu, P.; Gardner, S. *J. Am. Chem. Soc.* **2004**, *126*, 3378.
(7) McCulloch, I.; Heeney, M.; Bailey, C.; Genevicius, K.; Macdonald, I.; Shkunov, M.; Sparrowe, D.; Tierney, S.; Wagner, R.; Zhang, W.; Chabinyc, M. L.; Kline, R. J.; McGehee, M. D.; Toney, M. F. *Nature Mater.* **2006**, *5*, 328.

(8) Fong, H. H.; Pozdin, V. A.; Amassian, A.; Malliaras, G. G.; Smilgies, D.-M.; He, M.; Gasper, S.; Zhang, F.; Sorensen, M. *J. Am. Chem. Soc.* **2008**, *130*, 13202.
(9) Katz, H. E. *Chem. Mater.* **2004**, *16*, 4748.
(10) Allard, S.; Forster, M.; Souharce, B.; Thiem, H.; Scherf, U. *Angew. Chem., Int. Ed.* **2008**, *47*, 4070.
(11) (a) Kline, J.; DeLongchamp, M. D.; Fischer, A. D.; Lin, C. E.; Richter, J. L.; Chabinyc, L. M.; Toney, F. M.; Heeney, M.; McCulloch, I. *Macromolecules* **2007**, *40*, 7960–7965. (b) McCulloch, I.; et al. *Adv. Mater.* **2009**, *21*, 1091–1109.
(12) He, M.; Li, J.; Sorensen, M. L.; Zhang, F.; Hancock, R. R.; Fong, H. H.; Pozdin, V. A.; Smilgies, D.-M.; Malliaras, G. G. *J. Am. Chem. Soc.* **2009**, *131*, 11930.

Scheme 1. Molecular Structures of (a) P2TDC10FT*n* (*n* = 3, 4, 5) Polymers and (b) P*m*TDC13FT4 (*m* = 1, 2, 3) Polymers
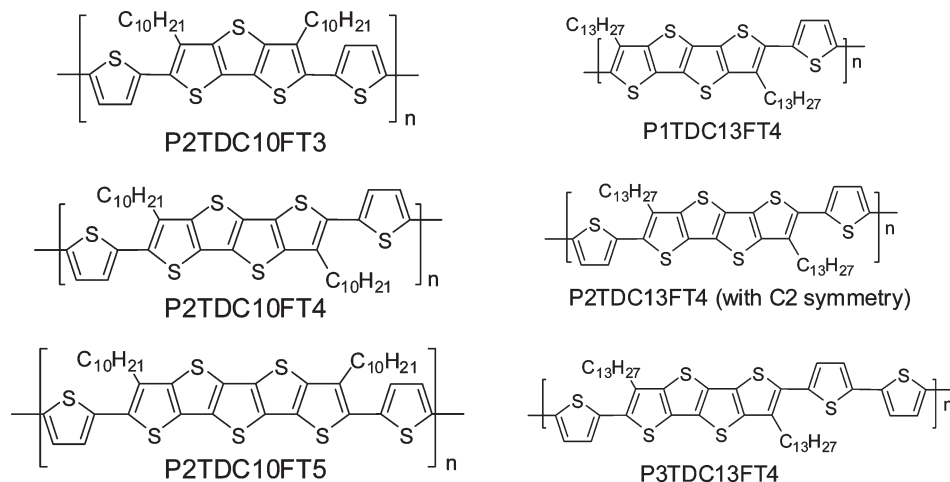
Scheme 2. Synthesis of P1TDC13FT4 and P3TDC13FT4 Polymers
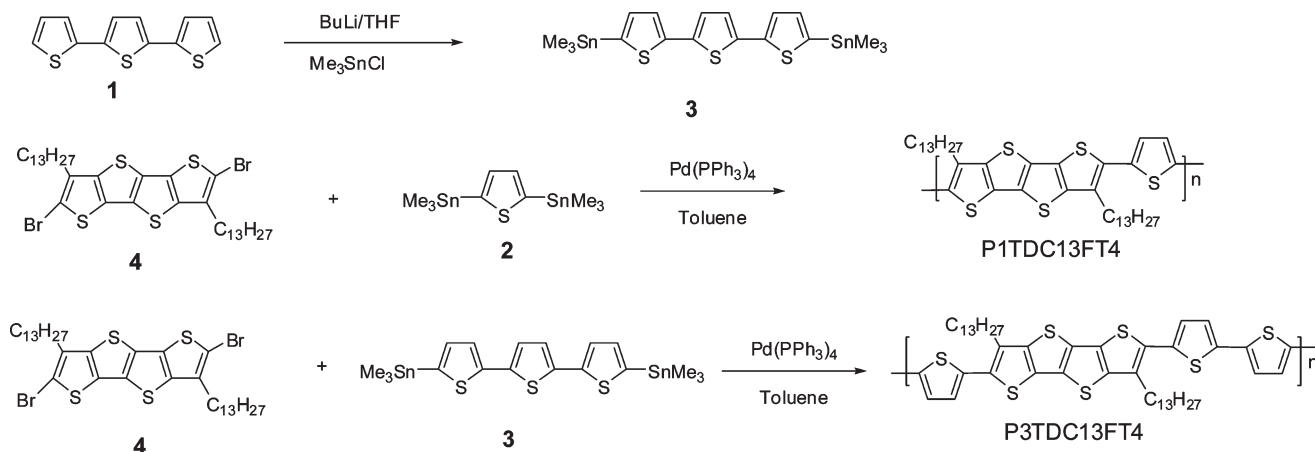
the properties of P2TDC10FT3, P2TDC10FT4, and P2TDC10FT5 (see structures above) indicated that the polymer with the even-numbered fused-thiophene core exhibits a much smaller lamellar spacing than the polymers featuring odd-numbered fused-thiophene cores. As a result, transistors fabricated from polymer with the even-numbered fused-thiophene core (P2TDC10FT4) yielded a much higher field-effect mobility than the other two (P2TDC10FT3 and P2TDC10FT5).[12] To obtain further insight into the structure−property relationships in polymeric semiconductors, we designed and synthesized two additional polymers in which we have kept the high-mobility 4-fold fused-thiophene core and varied the co-component part to monothiophene or terthiophene. The chemical structure of these two new polymers, P1TDC13FT4 and P3TDC13FT4, is shown in Scheme 1. Together with P2TDC13FT4, which is a polymer with a bithiophene co-component that was reported earlier,[8] they constitute a new family of polymers that can help elucidate the role of symmetry of the polymer repeat unit on structure and device performance.

Experimental Section

Polymer Synthesis. Poly(α-thienyl)-(3,7-ditridecanyltetrathieno-acene) (P1TDC13FT4) and poly(α-terthienyl)-(3,7-ditridecanyl-

tetrathienoacene) (P3TDC13FT4) were synthesized following Scheme 2. The detailed synthetic procedure is described in this scheme.

Compound **2** was synthesized and characterized by following the procedures described in ref 13.

1,1′-[2,2′:5′,2′′-terthiophene]-5,5′′-diylbis[1,1,1-trimethylstannane] (**3**). Butyl lithium (6.8 mL, 16.9 mmol) was added dropwise to terthiophene (2.0 g, 8.1 mmol) in dry tetrahydrofuran (THF) (100 mL) at −78 °C. The resulting mixture was slowly warmed to room temperature and cooled to −78 °C again before trimethyl tin chloride (16.9 mL, 16.9 mmol) was added. This mixture was stirred overnight and poured into saturated NaHCO₃ solution (100 mL). Organic was extracted with ethyl ether (2 × 100 mL) and washed with water (2 × 100 mL). The organic solution was dried over MgSO₄. After removal of the solvent, the solid was stirred in methanol (60 mL) and filtrated. The solid was then heated in ethanol (150 mL) and the upper clear solution was collected. The target compound was collected via crystallization and yielded 1.7 g of light yellow solid (36.8%). ^{1}H NMR: Solvent: methylene chloride, 7.28 (d, 2H), 7.11 (d, overlapped, 4H) and 0.39 (S, 18H).

Poly(α-thienyl)-(3,7-ditridecanyltetrathienoacene) (*P1TDC-13FT4*). 2,6-Dibromo-3,7-ditridecanyltetrathienoacene (0.61 g, 0.79 mmol) (**4**)[8] and 2,5-ditrimethyltinthiophene (0.32 g, 0.79 mmol) (**2**) were dissolved into toluene (20 mL) in a flask.

(13) Furuta, P.; Frechet, J. M. J. *J. Am. Chem. Soc.* **2003**, *125*, 13173.

Dry nitrogen was bubbled through this flask for a few minutes. Tetrakis(triphenylphosphine)palladium(0) (0.046 g, 0.04 mmol) was added to this mixture. The flask then was heated to 125 °C under nitrogen overnight before the content was poured into a methanol (200 mL) and concentrated hydrochloric acid (10 mL) solution and stirred overnight at room temperature. The precipitate was filtered and extracted in a Soxhlet with acetone and hexane for 24 h each. The collected polymer was dried under vacuum to yield 0.42 g (76.4%), with molecular weights of $M_n =$ 16 924, $M_w = 22\,690$ using GPC (1,2-dichlorobenzene). The polymer had two major absorption peaks at $\lambda_1 = 545$ nm and $\lambda_2 = 589$ nm (thin film). Anal. Calc. for $C_{40}H_{58}S_5$: C, 68.71; H, 8.36; S, 22.93. Found: C, 68.04; H, 8.87; S, 22.82.

Poly(α-terthienyl)-(3,7-ditridecanyltetrathienoacene) (*P3TDC-13FT4*). 2,6-Dibromo-3,7-ditridecanyltetrathienoacene (0.32 g, 0.38 mmol) (**4**)[8] and 1,1′-[2,2′:5′,2″-terthiophene]-5,5″-diylbis-[1,1,1-trimethylstannane] (0.22 g, 0.38 mmol) were dissolved into toluene (20 mL) in a flask. Nitrogen was bubbled through this flask for a few minutes. Tetrakis(triphenylphosphine)-palladium(0) (0.02 g, 0.19 mmol) was added to the mixture. The flask then was heated to 125 °C under nitrogen overnight before the content was poured into methanol (200 mL) and concentrated hydrochloric acid (10 mL) solution and stirred overnight at room temperature. The precipitate was filtered and extracted in a Soxhlet with acetone and hexane for 24 h each. The collected polymer was dried under vacuum to yield 0.28 g (77.8%) with molecular weights of $M_n = 10\,174$, $M_w = 11\,221$ using GPC (1,2-dichlorobenzene). The polymer had two major absorption peaks at $\lambda_1 = 545$ nm and $\lambda_2 = 589$ nm (thin film). Anal. Calc. for $C_{48}H_{62}S_7$: C, 66.77; H, 7.24; S, 25.99. Found: C, 66.01; H, 6.97; S, 26.82.

Characterization Measurements. Polymers were characterized by elemental analysis using a CE Elantech FlashEA 1112 Series CNHS-O analyzer. Polymer molecular weights were evaluated via gel permeation chromatography (GPC) using a Waters Alliance 2690 separation module with a Styragel HT3 column (4.6 × 300 mm, 10 μm, 500−30 000 molecular weight range) and a Styragel HT6E column (4.6 × 300 mm, 10 μm, 5000−10 000 000 molecular weight range) connected in series. Detection was completed by a Waters Model 2410 Refractive Index Detector and a Waters Model 996 Photodiode Array Detector. Calibrations were conducted with external polystyrene standards, Easi-Cal PS-2 A and B (Polymer Laboratories, Ltd.) at 0.1% w/v in toluene. The mobile phase was 1,2-dichlorobenzene with a flow rate of 0.5 mL/min and a column temperature of 35 °C. Samples were prepared at a concentration of 1 mg/mL in dichlorobenzene. Injection volume was 50 μL.

Structure and crystallinity of polymer films were analyzed using X-ray diffraction (XRD) with a Scintag diffractometer, employing a Cu target ($\lambda = 1.5405$ Å). A θ–2θ scan with a step size of 0.02° was set up between 2° and 12°, with scan rate of 0.02°/s. For X-ray measurements, polymers were spin-cast from pentachloroethane solution (3 mg/mL) on HMDS-treated SiO₂. These samples were further annealed at 150 °C for 10 min. Atomic force microscopy (AFM) was performed in tapping mode on a Digital Instruments Model DI-3000 apparatus.

Fabrication and Characterization of OFET Devices. Top-contact bottom-gate transistors using P*m*TDC13FT4 ($m = 1, 3$) as the organic semiconducting channel were fabricated under ambient conditions. Heavily doped Si ⟨1 0 0⟩ wafers were used as gate electrodes with a 300-nm thermally grown silicon dioxide layer as the gate dielectric. The substrates were cleaned by sonication in semiconductor-grade acetone and isopropanol, for 10 min in each solvent, and then they were given a 15-min air plasma treatment.

Table 1. GPC Characterizations of P1TDC13FT4 and P3TDC13FT4

polymer	M_n	M_w	polydispersity
P1TDC13FT4	16924	22690	1.34
P3TDC13FT4	10174	11221	1.10

Hexamethyldisilazane (HMDS, ≥99%) was used for surface modification of the gate dielectric layer. Prior to the SAM treatment, precleaned Si/SiO₂ samples were baked at 200 °C for 15 min in N₂ for dehydration.

Solutions of polymers in pentachloroethane (3 mg/mL) were prepared by heating to 170 °C for 30 min with stirring to speed up dissolution. Polymer films were then deposited by spin-coating at 1500 rpm for 40 s. The films were baked at 150 °C in a vacuum chamber to remove the solvent prior to thermal evaporation of top contacts. Gold contacts (50 nm) for source and drain electrodes were vacuum-deposited at a rate of 2.5 Å/s through a metal shadow mask that defined a series of transistor devices with a channel length (L) of 80 μm and a channel width (W) of 1 mm. Polymeric transistors were characterized in air using the Cascade Microtech Model 12861B probe station and Keithley Model 4200-SCS semiconductor characterization system.

When measuring current−voltage curves and transfer curves, the gate voltage (V_G) was scanned from +20 V to −80 V. The mobility was evaluated from the saturation regime with a source-drain voltage (V_{SD}) = −80 V, using the following equation:

$$I_{DS,sat} = \left(\frac{W}{2L}\right)\mu_i C_r (V_G - V_{TH})^2 \qquad (1)$$

where I_{DS} is the drain current, C_r the capacitance per unit area of the gate dielectric layer, V_G the gate voltage, and V_{TH} the threshold voltage. V_{TH} was determined from the intercept in the plot of $(I_{DS})^{1/2}$ vs V_G.

Results and Discussions

Molecular Weight. Gel permeation chromatography (GPC) was used to characterize the molecular weight of P1TDC13FT4 and P3TDC13FT4, using 1,2-dichlorobenzene as a solvent. Table 1 lists the results.

GPC results showed that P3TDC13FT4 gives narrower molecular weight distribution, with a polydispersity equal to 1.10. The P3TDC13FT4 polymer also exhibited a smaller molecular weight, which indicates the P3TDC13FT4 polymer has slightly lower solubility in the toluene system. However, both polymers are soluble enough to be dissolved into pentachloroethane for device fabrications.

UV−Vis Study. UV−vis studies were conducted to understand whether the P1TDC13FT4 and P3TDC13FT4 backbones are twisted. Both polymers were dissolved into chloroform, and their UV−vis spectra were compared to that of the P2TDC13FT4 polymer in Figure 1.[8]

P2TDC13FT4 and P3TDC13FT4 showed absorption maxima at 480 and 486 nm, respectively, while P1-TDC13FT4 showed an absorption maximum at 545 nm. Since the P2T and P3T polymers are linked by two and three single thiophene units with a single bond, they can rotate freely in solution, which results in shortening of the effective conjugation length. In the case of P1T, the rotational freedom is limited by the steric hindrance of the alkyl chains by the fused-thiophene ring system. The absorption maximum
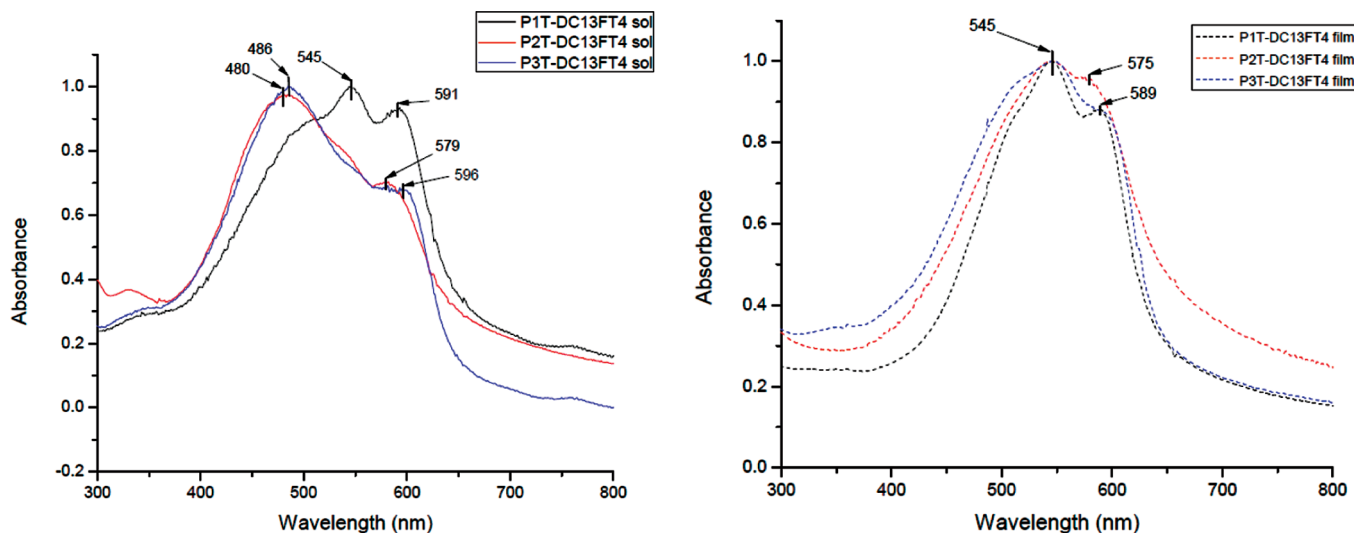
Figure 1. UV−vis of P1TDC13FT4, P2TDC13FT4, and P3TDC13FT4 in solution and solid state.

at 545 nm indicates a longer effective conjugation length. However, in the solid-state thin-film UV−vis, measurements for these three polymers yielded the same absorption maxima at 545 nm, with a shoulder peak at 589 nm for the P1TDC13FT4 and P3TDC13FT4 polymers and 575 nm for the P2TDC13FT4 polymer. These data indicate that conjugation along the polymer backbone is maintained, regardless of whether the polymer contains a single, bithiophene, or trithiophene unit as a co-component. The shift of the shoulder absorption of P1T and P3T to lower energies suggests that P1T and P3T are slightly better conjugated than the P2TDC13FT4 polymer.

Structure Characterization by X-ray Diffraction and AFM. In analyzing the diffraction patterns, we assume the previously observed polymer packing with lamella formation parallel to the substrate. From the recorded diffraction patterns (Figure 2), it is apparent that the lamellar spacing varies between samples, although the side-chain length remained constant. The lamellar spacings were determined to be 19.4, 18.7, and 24.5 Å for P1TDC13FT4, P2TDC13FT4, and P3TDC13FT4, respectively. The P3TDC13FT4 lamellar spacing is the biggest in this series of polymers, suggesting that, because of the lack of C_2 symmetry and, consequently, the side chains of adjacent fused backbones pointing in different directions, the close packing of vertically adjacent lamellae is inhibited.

The P1TDC13FT4 has a similar lamellae spacing to P2TDC13FT4, which possesses C_2 symmetry. This can be explained by considering the implication of a single thiophene ring between the fused-thiophene backbones along the P1TDC13FT4 polymer chain and the increased freedom of rotation around those bonds. It may be energetically favorable for the fused backbone and thiophene ring to rotate to reduce the hindrance of two closely located side chains pointing in the same direction, thereby resulting in side chains pointing in opposite directions and allowing close packing similar to P2TDC13FT4.

Using Scherrer analysis, we determined the average lamellar stack heights to be 11.4, 9.0, and 7.2 lamellae,
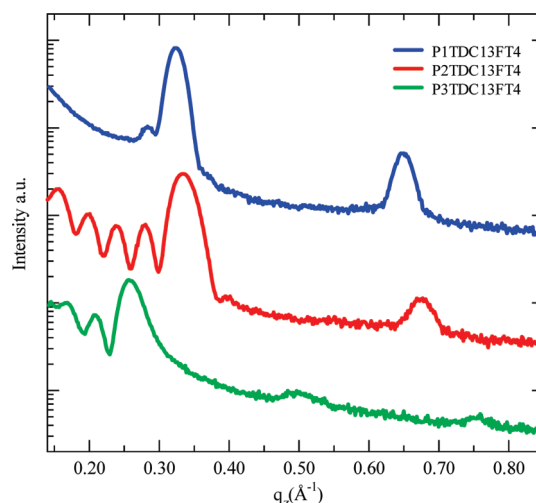

Figure 2. X-ray diffraction (XRD) patterns of P*n*TDC13FT4 films (*n* = 1, 2, 3).

respectively, which confirms that the P3TDC13FT4 film has the worst lamellar correlation, while P1TDC13FT4 and P2TDC13FT4 have similar ordering.

Additional features of the XRD measurement are the Laue oscillations close to the (100) peak in P2TDC13FT4 and P3TDC13FT4, which arise from a finite number of lamellae in the film. The presence of these oscillations suggests higher film ordering in the case of P2TDC13FT4 and P3TDC13FT4, as compared to P1TDC13FT4, where only one oscillation can be seen. The Laue oscillations yield an alternative determination of the lamellar stack height. From the oscillations, we are able to determine the lamellae stack height to be 8.5 and 5.8 lamellae for P2TDC13FT4 and P3TDC13FT4, respectively, which are similar to the results of the Scherrer analysis. The Laue oscillations are a direct measure of the average stack height variation, hence, the P2 and P3 films seem to consist of a quite narrowly determined number of lamellae, whereas in the P1 film, the number of lamellae in the film has a wider spread.

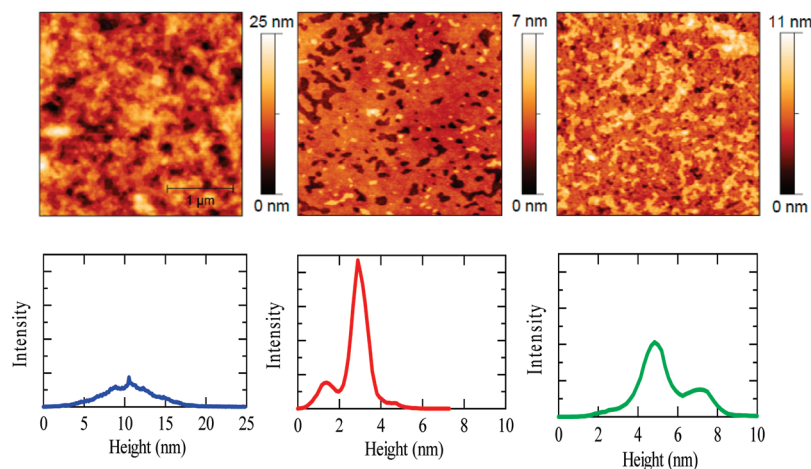AFM was utilized to study the topography of the polymer films. In the case of P2TDC13FT4 and P3TDC13FT4,

Figure 3. AFM images and associated height distribution functions of P*n*TDC13FT4 films (*n* = 1, 2, 3, from left to right). P2TDC13FT4 and P3TDC13FT4 show a clear lamellar structure with terraces, as also confirmed by the narrow height distributions featuring two prominent heights. The P1TDC13FT4 film features a much rougher surface.
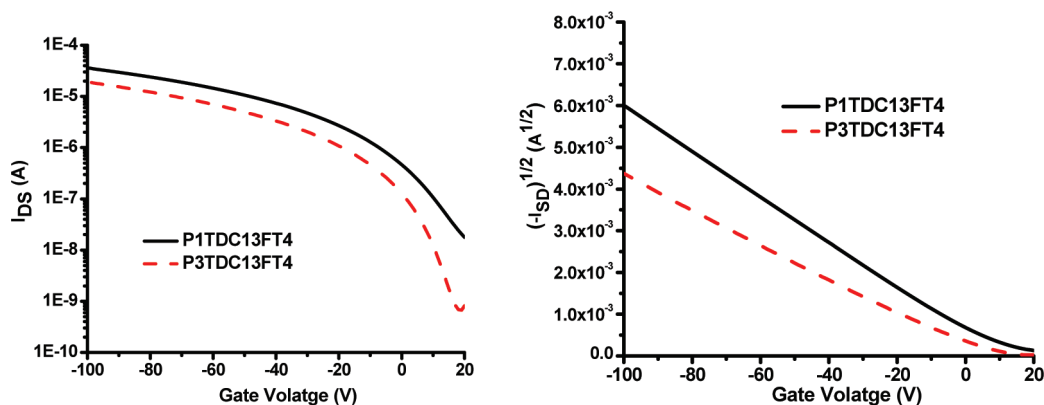

Figure 4. Transfer characteristics of the annealed polymer devices on HMDS-treated SiO_2/Si for P1TDC13FT4 and P3TDC13FT4 at V_{SD} = −80 V.

where more ordered lamellae are expected based on the XRD analysis, the topography reveals a terraced lamellae formation similar to PBTTT.[11a] (See Figure 3.) In contrast, P1TDC13FT4 has a much rougher topography, reminiscent of P3HT films, with no clearly discernible lamellar terraces. The average terrace diameter of the P2TDC13FT4 film is significantly higher than that for P3TDC13FT4, producing smoother films, which would be favorable for lateral charge transport. Through XRD and AFM analysis for these three polymers, the importance of C_2 symmetry begins to emerge. Hindrance that is due to lack of C_2 symmetry causes increased lamellae spacing, decreasing the π-system delocalization, as seen in the case of P3TDC13FT4. In contrast, P1TDC13FT4 films have a rougher appearance and much less well-organized lamellae. This higher degree of disorder due to the lack of C_2 symmetry seems to be the limiting factor in the observed mobility. The P2 polymer with C_2 symmetry seems to have the best of both worlds, with a small lamellar spacing and well-formed lamellar order, yielding significantly higher mobility.

Device Performance. The OFET properties of the polymers were evaluated using top contact devices fabricated by spin-casting the room-temperature pentachloroethane solution of the polymers on SiO_2 gate dielectrics, which

were treated by hexamethyldisilazane (HMDS). Figures 4 and 5 show the typical current−voltage characteristics of polymeric OFET devices with a channel length of L = 80 μm, where I_{SD}, V_{SD}, and V_G represent source-drain current, source-drain voltage, and gate voltage, respectively. The saturation region field-effect mobility (μ) was calculated from the transfer characteristics of the OFETs using the slope derived from $(-I_{SD})^{1/2}$ versus V_G plots between −100 V and −60 V (see Figure 4). The threshold voltages (V_{TH}) of different polymer OFETs were derived from the onset of the transfer curves.

The output curves (Figure 5) of polymers with different number of thiophene co-components show good saturation and linear behavior in the lower V_{SD} range. The linearity of the output curves in the low V_{SD} regime (0 V to −5 V) indicates that gold forms an ohmic contact with polymers. Mobility values, on/off ratios, and threshold voltages of the polymer devices for P1TDC13FT4 and P3TDC13FT4 on HMDS-treated SiO_2 surfaces are summarized in Table 2. All polymer devices showed very good reproducibility and low deviation values, which indicates the excellent uniformity of the polymer thin films. OFET characteristics of polymers on HMDS-treated surfaces are shown in Figures 4 and 5.
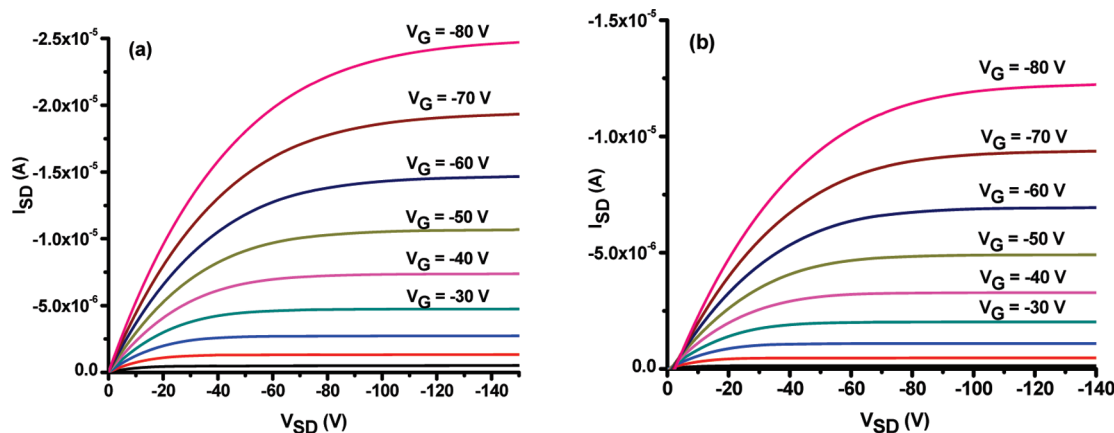
Article

Chem. Mater., Vol. 22, No. 9, 2010 **2775**

Figure 5. Output curves of the annealed polymer devices on HMDS-treated SiO_2/Si for (a) P1TDC13FT4 and (b) P3TDC13FT4 at different gate voltages.

Table 2. Device Performance of the P1TDC13FT4 and P3TDC13FT4 Polymers on HMDS-Treated SiO_2/Si

polymer	maximum mobility, μ_{max} (cm^2/(V s))	average mobility of 40 devices, $\mu_{average}$ (cm^2/(V s))	deviation (cm^2/(V s))	on/off ratio	V_t (V)
P1TDC13FT4	0.0479	0.0421	0.00532	10^3–10^4	10
P3TDC13FT4	0.0269	0.0226	0.00171	10^4–10^5	5

Table 2 shows that the P1TDC13FT4 polymer gave higher mobility values than that of the P3TDC13FT4 polymer. However, the 0.048 cm^2/(V s) mobility values obtained from HMDS-treated surfaces are ~6 times smaller than our reported value of 0.33 cm^2/(V s) for P2TDC13FT4.[8] On the other hand, the P3TDC13FT4 polymers exhibited mobility values that were one order of magnitude lower than those of the P2TDC13FT4 polymer.

Symmetry and Mobility. Combined with our previous device performance study, we have investigated the transport properties for two series of fused-thiophene copolymers. In the first case, we characterized a family of P2TDC10FT3, P2TDC10FT4, and P2TDC10FT5 polymers in a recently reported family of thienoacene copolymers.[12] In this report, we have further characterized two more polymers—P1TDC13FT4 and P3TDC13FT4—to compare with our previous published P2TDC13FT4 data. In the first series, the length of the fused core was systematically increased from three to four to five units, leading to an increase in the backbone rigidity, while the length of the alkyl side chains was kept constant to facilitate comparisons between the three polymers. In the second case, the four-member fused core was maintained, while the co-component part was changed from bithiophene to include single thiophene and terthiophene moieties. In the first series, devices made from the polymer with the four fused rings (P2TDC10FT4) showed a hole mobility of 0.087 cm^2/(V s), whereas devices made from the polymers with the three fused rings (P2TDC10FT3) and five fused rings (P2TDC10FT5) showed hole mobilities of 0.0017 and 0.0023 cm^2/(V s), respectively. Devices made from P1TDC13FT4 and P3TDC13FT4 showed a hole mobility of 0.042 and 0.022 cm^2/(V s), respectively, which is ~1 order of magnitude lower than the 0.33 cm^2/(V s) value achieved with P2TDC13FT4.[8]

The fact that the performance of P2TDC10FT5 is an order of magnitude lower than that of P2TDC10FT4 is surprising. In the context of semiclassical electron-transfer theory, the Marcus model of charge transfer suggests an increase of the hopping rate with decreasing reorganization energies. Calculations with Gaussian 03 using BL3YP/6-31G** show that a five-fused-ring small molecule has lower reorganization energy than a four-fused-ring one (see the Supporting Information). Therefore, with all else being equal, a higher mobility would be expected in P2TDC10FT5.[14] Moreover, one would expect that the increase in the length of the rigid core from four fused rings to five fused rings would lead to better packing and, hence, lead to a higher mobility. As opposed to this expectation, synchrotron X-ray scattering shows that both P2TDC10FT3 and P2TDC10FT5 show poor lamellar packing, in contrast with P2TDC10FT4, which shows good lamellae formation and in-plane order, as well as a much smaller lamellar spacing.[12]

Our data show that packing and mobility depend on whether the number of fused rings or co-components is odd (low mobility) or even (high mobility). This variation affects not only the length of the rigid core, but also the relative location of the side chains, with respect to the polymer backbone. In fact, the side chains in P2TDC10FT3 and P2TDC10FT5 are on the same side of the conjugated core, whereas, in P2TDC10FT4, they are on opposite sides. This means that the relative arrangement of side chains, rather than the length of the rigid core, dominates chain packing in the film.

In the second case, of P1TDC13FT4 and P3TDC-13FT4 polymers, we have kept the FT4 core and, thus, avoided the direction change of the substituted alkyl

(14) Coropceanu, V.; Malagoli, M.; da Silva Filho, D. A.; Gruhn, N. E.; Bill, T. G.; Brédas, J. L. *Phys. Rev. Lett.* **2002**, *89*, 275503.
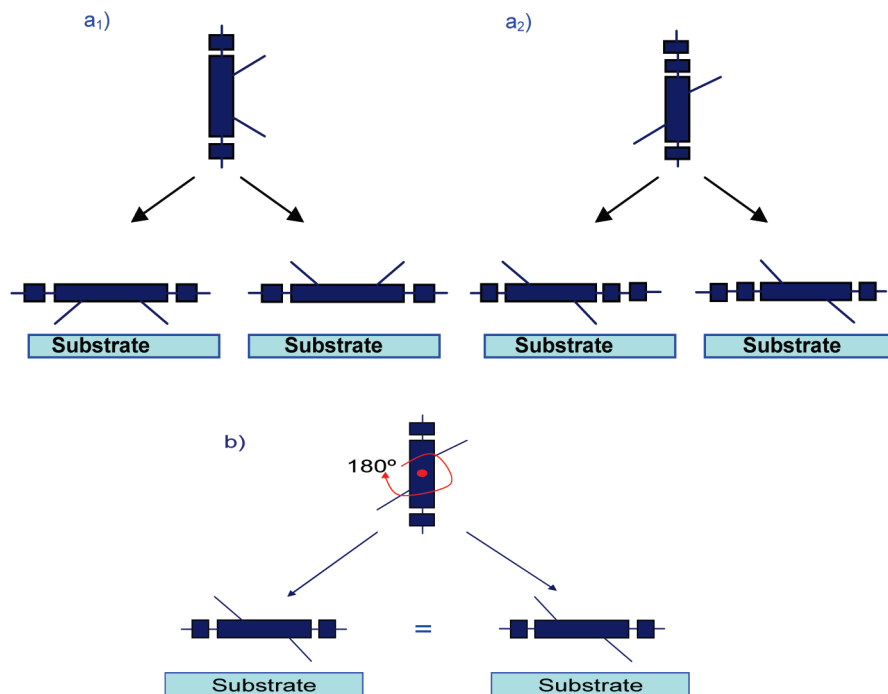
Figure 6. Possible configurations of the repeat unit with respect to the substrate, for repeat units (a_1 and a_2) without and (b) with C_2 symmetry. Judging from the family of closely related conjugated polymers that we have investigated, C_2 symmetry seems to enable a very small lamellar period and promote high mobility.

groups. Changing the bithiophene co-unit to a single thiophene and terthiophene switched the even number of connecting thiophene moieties to odd numbers, and significant mobility decreases were observed .This decrease in mobility cannot be explained by a breakdown of the extended conjugation, because the UV−vis spectra of the P1TDC13FT4 and P3TDC13FT4 polymer thin films show almost no changes, compared to that of P2TDC13FT4.[8] The reason for this behavior becomes clear if one thinks in terms of the symmetry of the repeat unit, as Figure 6 aims to illustrate.

In the first case, upon spin coating, the polymer chains arrange parallel to the substrate. This process is, to first order, random, and will lead to a distribution of orientations of the side chains with respect to the substrate. If both side chains are on the same side of the backbone (Figure $6a_1$), the two possible configurations of side chains pointing toward the substrate and side chains pointing away from the substrate will be different. Similarly, an asymmetry in a co-monomer unit (Figure $6a_2$) will yield two distinct configurations when the polymer chains arrange parallel to the substrate. However, if the side chains are arranged in such a fashion so that the repeat unit possesses a C_2-axis perpendicular to the conjugation plane (Figure 6b), the two possible configurations will be equivalent. This will clearly aid in the packing of main chains. Moreover, we found that the packing of the main chains is intimately related to achieving high mobility.

It is interesting to raise the question whether the experimental results presented here would constitute a general design rule. Such a rule cannot possibly be suggested using examples from only a single polymer family. However, the literature seems ripe with data that support this C_2 symmetry design rule. One example is a

pair of thienothiophene copolymers, pBTTT and pBTCT, reported by McCulloch, Heeney, and co-workers.[11,15] The repeat unit of pBTTT shows C_2 group symmetry with the "anti" positioning of the S atoms in the thieno[3,2-b]thiophene monomer. In contrast to pBTTT, pBTCT shows no C_2 symmetry, yielding a mobility of only 0.03 cm^2/(V s), over an order of magnitude lower than the reported mobility for pBTTT. Aside from PQT-12, pBTTT, and P2TDC13FT4, several polymer semiconductors that exhibit a hole mobility of >0.1 cm^2/(V s) were reported recently, including PTzQTs-R,[16] PQTBTz-C12,[17] PETV12T,[18] and poly(4,8-dialkyl-2,6-bis(3-alkylthiophen-2-yl)benzo[1,2-b:4,5-b′]dithiophene) (the latter of which is a benzodithiophene copolymer).[19] As shown in Table 3, the repeat units of these polymers exhibit C_2 symmetry, supporting the C_2 rule proposed here.

Moreover, the recently reported *n*-type polymer poly{[*N*, *N*′-bis(2-octyldodecyl)-naphthalene-1,4,5,8-bis(dicarboximide)-2,6-diyl]-alt-5,5′-(2,2′-bithiophene)} {P(NDI2OD-T2)}, which shows a high electron mobility (0.1−0.85 cm^2/(V s))[20] also has a repeat unit that shows C_2 symmetry.

(15) Heeney, M.; Bailey, C.; Genevicius, K.; Shkunov, M.; Sparrowe, D.; Tierney, S.; McCulloch, I. *J. Am. Chem. Soc.* **2005**, *127*, 1078.
(16) Osaka, I.; Zhang, R.; Sauvé, G.; Smilgies, D. -M.; Kowalewski, T.; McCullough, R. D. *J. Am. Chem. Soc.* **2009**, *131*, 2521.
(17) Kim, D. H.; Lee, B.-L.; Moon, H.; Kang, H. M.; Jeong, E. J.; Park, J.-I.; Han, K.-M.; Lee, S.; Yoo, B. W.; Koo, B. W.; Kim, J. Y.; Lee, W. H.; Cho, K.; Becerril, H. A.; Bao, Z. *J. Am. Chem. Soc.* **2009**, *131*, 6124.
(18) Lim, B.; Baeg, K.-J.; Jeong, H.-G.; Jo, J.; Kim, H.; Park, J.-W.; Noh, Y.-Y.; Vak, D.; Park, J.-H.; Park, J.-W.; Kim, D.-Y. *Adv. Mater.* **2009**, *21*, 2808.
(19) Pan, H; Li, Y.; Wu, Y.; Liu, P.; Ong, B. S.; Zhu, S.; Xu, G. *J. Am. Chem. Soc.* **2007**, *129*, 4112.
(20) Yan, H.; Chen, Z.; Zheng, Y.; Newman, C.; Quinn, J. R.; Dötz, F.; Kastler, M.; Facchetti, A. *Nature* **2009**, *457*, 679.

Table 3. High-Performance Semiconducting Polymers and the Symmetry of Their Repeating Units
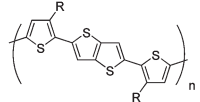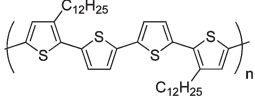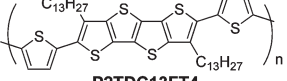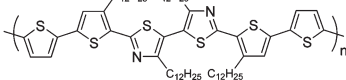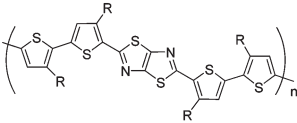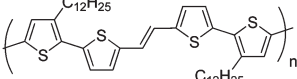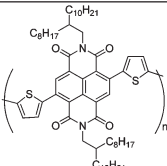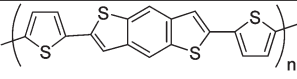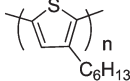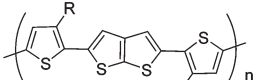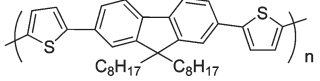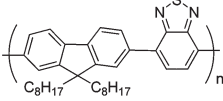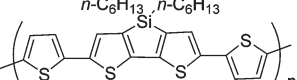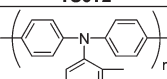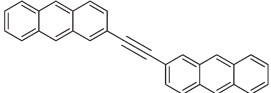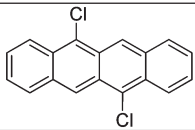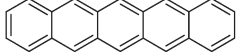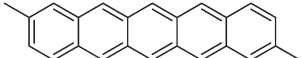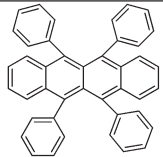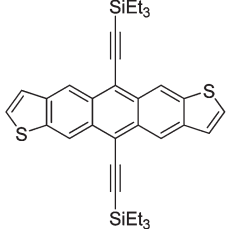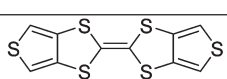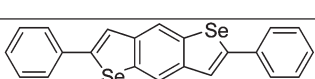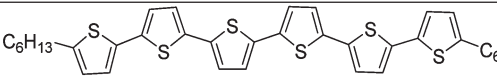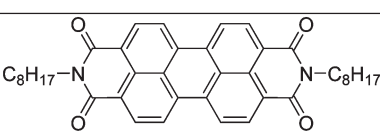
Materials	Field-Effect Mobility [cm^2 / (V·s)]	C$_2$ Symmetry	Reference
PBTTT	0.2-0.6 (holes)	Yes	7
PQT-12	0.06-0.12 (holes)	Yes	6
P2TDC13FT4	0.18-0.33 (holes)	Yes	8
PQTBTz-C12	0.33 (holes)	Yes	17
PTzQT-R	0.01-0.3 (holes)	Yes	16
PETV12T	0.15 (holes)	Yes	18
P(NDI2OD-T2)	0.1-0.85 (electrons)	Yes	20
Benzodithiophene copolymer	0.15-0.25 (holes)	Yes	19
P3HT	0.01-0.1 (holes)	No	3
PBTCT	0.03 (holes)	No	15
F8T2	0.001-0.01 (holes)	No	21
F8BT	0.001 (electrons)	No	22
TS6T2	0.08 (holes)	No	23
PTAA	0.003 (holes)	No	24

Table 4. High-Mobility Semiconducting Small Molecules

Materials	Field-Effect Mobility [cm^2 / (V·s)]	Symmetry	References
	1.1 (holes)	C$_2$	26
	1.6 (holes)	C$_2$	27
	6 (holes)	C$_2$	28
	2.5 (holes)	C$_2$	29
	15.4 (holes)	C$_2$	30
	1 (holes)	C$_2$	31
	1.4 (holes)	C$_2$	32
	1.5 (holes)	C$_2$	33
	1.1 (holes)	C$_2$	34
	1.3 (electrons)	C$_2$	35

The question arises whether this C_2 rule is also applicable to small molecules. A quick review of structures in the *Organic Field-Effect Transistors* book by Bao and Locklin indicates that molecules with a mobility of > 1.0 cm^2/(V s) fulfilled the C_2 rule, out of a set of more than 400 molecules.[25] Table 4 highlights such reported high-mobility

structures. However, since small molecules can rearrange during crystallization much easier than polymers, the C_2 symmetry rule is more important for the latter class of materials.

We also need to note the exceptions to the C_2 rule. First of all, the prototypical conjugated polymer regioregular

(21) Sirringhaus, H.; Wilson, R. J.; Friend, R. H.; Inbasekaran, M.; Wu, W.; Woo, E. P.; Grell, M.; Bradley, D. D. C. *Appl. Phys. Lett.* **2000**, *77*, 406.
(22) Donley, C. L.; Zaumseil, J.; Andreasen, J. W.; Nielsen, M. M.; Sirringhaus, H.; Friend, R. H.; Kim, J.-S. *J. Am. Chem. Soc.* **2005**, *127*, 12890.
(23) Lu, G.; Usta, H.; Risko, C.; Wang, L.; Facchetti, A.; Ratner, M. A.; Marks, T. J. *J. Am. Chem. Soc.* **2008**, *130*, 7670.
(24) Veres, J.; Ogier, S. D.; Leeming, S. W.; Cupertino, D. C.; Khaffaf, S. M. *Adv. Funct. Mater.* **2003**, *13*, 199.
(25) *Organic Field-Effect Transistors*, 1st ed.; Bao, Z., Locklin, J., Eds.; CRC Press: Boca Raton, FL, 2007; pp 203−213.

(26) Gerlach, C. P.; Kelley, T. W.; Muyres, D. V. Presented at the 227th ACS National Meeting, Anaheim, CA, 2004.
(27) Moon, H.; Zeis, R.; Borkent, E.-J.; Besnard, C.; Lovinger, A. J.; Siegrist, T.; Kloc, C.; Bao, Z. *J. Am. Chem. Soc.* **2004**, *126*, 15322.
(28) Kelley, T. W.; Muyres, D. V.; Baude, P. F.; Smith, T. P.; Jones, T. D. *Mater. Res. Soc. Symp. Proc.* **2003**, *771*, 169.
(29) Kelly, T. W.; Boardman, L. D.; Dunbar, T. D.; Muyres, D. V.; Pellerite, M. J.; Smith, T. P. *J. Phys. Chem. B* **2003**, *107*, 5877.
(30) Sundar, V. C.; Zaumseil, J.; Podzorov, V.; Menard, E.; Willett, R. L.; Someya, T.; Gershenson, M. E.; Rogers, J. A. Science **2004**, *303*, 1644.

Article

Chem. Mater., Vol. 22, No. 9, 2010 2779

P3HT is the most marked exception. Tsao et al. reported a cyclopentadithiophene−benzothiadiazole polymer with a mobility of 1.3 cm^2/(V s) through a slow dip-coating process,[36] while Guo et al. reported a PhBT polymer with mobility of 0.2 cm^2/(V s).[37] Note that the slow dip-coating method used to form films is similar to a crystal growing process and yields films that are better ordered (and, hence, have fewer defects) than spin-coated ones.[38] Furthermore, Bao's group also reported a thienopirazine−fluorene copolymer with a maximum field-effect mobility of 0.2 cm^2/(V s).[39] Also note that these latter three exceptions are donor−acceptor structures. In these cases, the thin-film formation process may strongly be influenced by dipole interactions and the charge carrier transport mechanism may be different from the symmetric molecules and polymers. This raises the tantalizing prospect that such functionalities and advanced deposition methods offer new ways to tune structure−property relationships.

Conclusion

The relationship between molecular structure and field-effect mobility was investigated in a family of fused-ring thiophene copolymers. The results strongly suggest a correlation between a repeat unit that possesses a C_2-axis perpendicular to the conjugation plane, a minimum attainable lamellar spacing, and a high field-effect mobility. Both our experimental results and combined literature survey supports this suggestion: Although a few notable exceptions to this rule have been identified, C_2 symmetry seems to pave the way to high-mobility polymers.

Supporting Information Available: Synthesis, experimental procedures; characterizations and complete author list for ref 11b. This material is available free of charge via the Internet at http://pubs.acs.org.

(31) Payne, M. M.; Parkin, S. R.; Anthony, J. E.; Kuo, C.-C.; Jackson, T. N. *J. Am. Chem. Soc.* **2005**, *127*, 4986.
(32) Mas-Torrent, M.; Durkut, M.; Hadley, P.; Ribas, X.; Rovira, C. *J. Am. Chem. Soc.* **2004**, *126*, 984.
(33) Zeis, R.; Kloc, C.; Takimiya, K.; Kunugi, Y.; Konda, Y.; Niihara, N.; Otsubo, T. *Jpn. J. Appl. Phys.* **2005**, *44*(Part 1), 3712.
(34) Halik, M.; Klauk, H.; Zschieschang, U.; Schmid, G.; Ponomarenko, S.; Kirchmeyer, S.; Weber, W. *Adv. Mater.* **2003**, *15*, 917.
(35) Chesterfield, R. J.; McKeen, J. C.; Newman, C. R.; Ewbank, P. C.; Da Silva Filho, D. A.; Bredas, J.-L.; Miller, L. L.; Mann, K. R.; Frisbie, C. D. *J. Phys. Chem. B* **2004**, *108*, 19281.
(36) Tsao, H. N.; Cho, D.; Andreasen, J. W.; Rouhanipour, A.; Breiby, D. W.; Pisula, W.; Müllen, K. *Adv. Mater.* **2009**, *21*, 209.
(37) Guo, X.; Kim, F. S.; Jenekhe, S. A.; Watson, M. D. *J. Am. Chem. Soc.* **2009**, *131*, 7206.
(38) Park, S. K.; Jackson, T. N.; Anthony, J. E.; Mourey, D. A. *Appl. Phys. Lett.* **2007**, *91*, 063514.
(39) Becerril, H. A.; Miyaki, N.; Tang, M. L.; Mondal, R.; Sun, Y.-S.; Mayer, A. C.; Parmer, J. E.; McGehee, M. D.; Bao, Z. *J. Mater. Chem.* **2009**, *19*, 591.